

EUROPEAN ORGANIZATION FOR NUCLEAR RESEARCH

Proposal to the ISOLDE and Neutron Time-of-Flight Committee

Detailed decay spectroscopy of  $^{225}\text{Ac}$  and its daughters to support its use in medical applications

September 26, 2023

A. Algora<sup>1</sup>, A.N. Andreyev<sup>2</sup>, S. Bara<sup>3</sup>, S. Benzoni<sup>4</sup>, T.E. Cocolios<sup>3</sup>, S.M. Collins<sup>5,6</sup>, C. Costache<sup>7</sup>, J. Cubiss<sup>2</sup>, U. Datta Pramanik<sup>8</sup>, H. De Witte<sup>3</sup>, D.T. Doherty<sup>6</sup>, Z. Favier<sup>9</sup>, W. Gelletly<sup>6</sup>, J. Heery<sup>5,6</sup>, J. Henderson<sup>6</sup>, M. Heines<sup>3</sup>, A. Illana Sison<sup>10</sup>, E. Jajčíšínová<sup>1</sup>, J.D. Johnson<sup>3</sup>, P. Jones<sup>12</sup>, R. Lica<sup>7</sup>, C. Mihai<sup>7</sup>, E. Nacher<sup>13</sup>, E.B. O’Sullilvan<sup>5,6</sup>, B. Olaizola Mampaso<sup>14</sup>, S.G. Pascu<sup>6,7</sup>, S. Poulton<sup>5,6</sup>, P.H. Regan<sup>5,6</sup>, c. Page<sup>2</sup>, Zs. Podolyak<sup>6</sup>, M. Polettini<sup>15</sup>, R. Shearman<sup>5</sup>, C. Sotty<sup>7</sup>, A. Stoica<sup>7</sup>, M. Stryjczyk<sup>16</sup>, A. Turturica<sup>7</sup>, P. Van Duppen<sup>3</sup>, W. Wojtaczka<sup>3</sup>, Z. Yue<sup>2</sup>

<sup>1</sup>*IFIC, Valencia, Spain*

<sup>2</sup>*The University of York, York, United Kingdom* <sup>3</sup>*KU Leuven, Institute for Nuclear and Radiation Physics, Leuven, Belgium*

<sup>4</sup>*INFN Milano, Milano, Italy*

<sup>5</sup>*National Physical Laboratory, Teddington, United Kingdom*

<sup>6</sup>*University of Surrey, Guildford, United Kingdom*

<sup>7</sup>*IFIN-HH, Bucharest, Romania*

<sup>8</sup>*Saha Institute of Nuclear Physics, Kolkata, India*

<sup>9</sup>*CERN, ISOLDE, Switzerland*

<sup>10</sup>*Grupo de Física Nuclear & IPARCOS, Universidad Complutense Madrid, Madrid, Spain*

<sup>11</sup>*Joint Research Center, European Commission, Karlsruhe, Germany*

<sup>12</sup>*iThemba LABS, Western Cape, South Africa*

<sup>13</sup>*Insituto de Física Corpuscular, CSIC, Madrid, Spain*

<sup>14</sup>*Insituto de Estructura de la Materia, CSIC, Madrid, Spain*

<sup>15</sup>*Universita’ degli Studi e INFN Padova, Padova, Italy*

<sup>16</sup>*University of Jyväskylä, Finland*

**Spokesperson:** Thomas Elias Cocolios, thomas.elias.cocolios@cern.ch

**Co-spokesperson:** Patrick Regan, p.regan@surrey.ac.uk

**Co-spokesperson:** Sean Collins, sean.collins@npl.co.uk

**Co-spokesperson:** Razvan Lica, razvan.lica@cern.ch

**Contact person:** Charlotte Duchemin, charlotte.duchemin@cern.ch



**Abstract:**  $^{225}\text{Ac}$  and  $^{213}\text{Bi}$  have been proposed as promising radioisotopes for targeted alpha therapy against metastasised cancers. However, the accuracy and precision of the knowledge of the decay properties of these isotopes and all those in their decay chain are currently not sufficient to reliably use them for large-scale medical applications. In the current proposal, we will measure the unique decay signatures of  $^{225}\text{Ac}$ ,  $^{221}\text{Fr}$ ,  $^{213}\text{Bi}$  and  $^{209}\text{Tl}$  using the ISOLDE Decay Station, thereby improving the knowledge of branching ratios in the  $\gamma$ -ray emissions and the transition multipolarities of definitive  $\gamma$ -ray cascades which are crucial nuclear data inputs required for the precise determination of absolute activities of radioactive materials, and ultimately determine the personal dosimetry during treatment.

**Requested shifts:** 3.5 shifts, (split into 3 runs over 1 to 2 years)

# 1 Targeted Alpha Therapy with $^{225}\text{Ac}$ and $^{213}\text{Bi}$

Cancer is one of the main causes of adult mortality, and as such the source for much research worldwide. Within Horizon Europe, the European Commission has even made *Beating Cancer* one of its main pillars, in order to support the research in the prevention, diagnostics, and treatment of cancer. An important field of research in this framework is nuclear medicine, where a targeted radioisotope is delivered in the body and aimed at monitoring body functions (e.g. sugar intake) by using either the natural affinity of the element (e.g. iodine for thyroid cells) or binding it to a molecule with a specific target (e.g. sugar derivative, receptor analog). The choice of radioisotope determines the purpose of the radiopharmaceutical: diagnostics is performed with  $\gamma$ -ray emitters of low energy (SPECT imaging) or with positron emitters (PET imaging); therapy is performed with charged particle emitters, mostly  $\beta^-$  but also  $\alpha$ .

Targeted Alpha Therapy (TAT) is the field of nuclear medicine dedicated to the treatment of cancer with  $\alpha$  emitters. Thanks to its high mass, the  $\alpha$  particle deposits more energy per unit path length than a  $\beta^-$  particle, causing more damage in a more localised region, which is coined as higher linear energy transfer (LET). The high LET of  $\alpha$  particles results in a high concentration of DNA damage in cells, increasing the probability for cell death. This is a clear advantage when reaching cancer cells, but can also be a high risk to healthy cells [1]. This duality has thus slowed the progress of TAT compared to other forms of radionuclide therapy, so that there is today only one drug used in the treatment of bone metastases in castration-resistant prostate cancers, using  $^{223}\text{Ra}$  for its natural affinity to calcium-seeking cells [2, 3].

Radiopharmaceuticals based on cell-specific receptors require a radiometal that may be chemically linked to the complex vector molecule, which is not possible with  $^{223}\text{Ra}$ . The radioisotope must also be accessible for production, have a half-life that can reasonably allow its manipulation and matches the biological lifetime of the molecule in the body<sup>1</sup>, have a substantial  $\alpha$ -decay branching ratio, and which progeny that do not present a risk to the patient.  $^{225}\text{Ac}$  ( $T_{1/2} \sim 10$  days) and  $^{213}\text{Bi}$  ( $T_{1/2} \sim 45$  min) have been identified as two such radioisotopes and have thus been the source of investigations in the last decades [4, 5, 6]. The short half-life of  $^{213}\text{Bi}$  can be overcome by its presence in the decay chain of  $^{225}\text{Ac}$ , through which generators can be made with a long shelf life and the possibility to elute a sample multiple times per day [7].

The recent success of  $^{225}\text{Ac}$ -PSMA-617 in the treatment of metastasised castration-resistant prostate cancer has shown the high potential of  $^{225}\text{Ac}$  for TAT [8, 9]. Together with the prospects offered by  $^{213}\text{Bi}$  [6], this has triggered a very strong effort towards achieving a reliable supply of these isotopes at large scale [10]. In particular, CERN contributes to this effort via its research performed at ISOLDE [11] and at MEDICIS [12, 13]. However, besides the supply reliability and the nuclear medicine application, many questions remain before their regular clinical use, in particular regarding their decay properties.

---

<sup>1</sup>From hours for very small molecules like peptides, to days for very large molecules like antibody fragments.

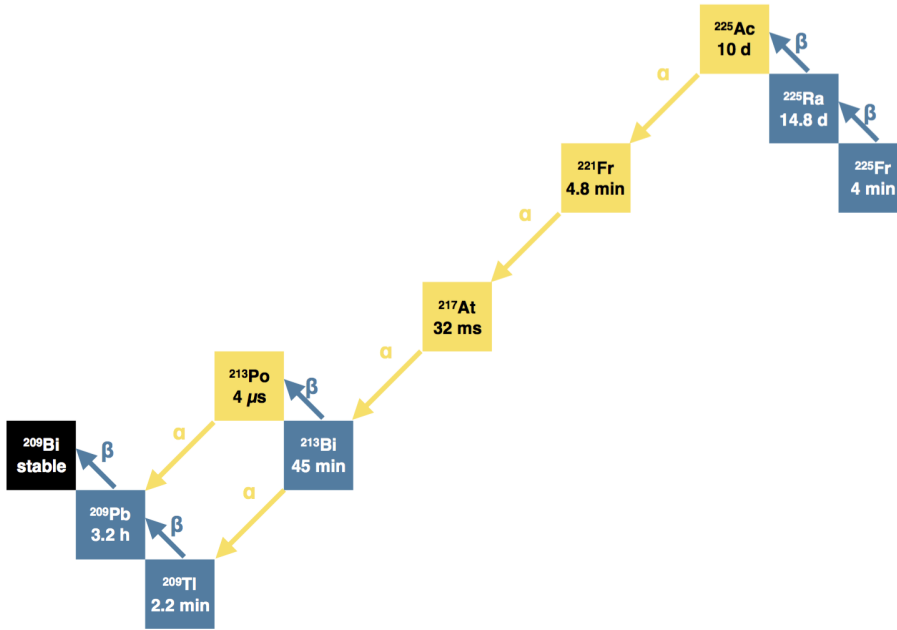


Figure 1: Decay chain from  $^{225}\text{Fr}$  to  $^{209}\text{Bi}$ , highlighting the half-life of each isotope and their main decay modes.

## 2 Decay of $^{225}\text{Ac}$ and its daughters

The decay properties of  $^{225}\text{Ac}$ ,  $^{213}\text{Bi}$ , and the other isotopes involved in their decay chain (see Fig. 1) are of high importance to TAT as they impact directly the dose delivered to the patients, but also because those properties are used to assess the production and processing efficiencies, or qualify the radioisotopes at different stages such as during transport from the production facility to the medical treatment facility. The most important properties are the half-lives, branching ratios in decay modes, and  $\gamma$ -ray emissions. The long half-life of  $^{225}\text{Ac}$  by standards of a radioactive ion beam facility would lead one to expect that the half-life has been well studied, however it had to be remeasured recently in order to obtain a sufficiently accurate and precise value for its use in medical settings [14], resulting in a reduction of the half-life by nearly 1% and the first determination of the uncertainty of this half-life.

Nonetheless, a thorough investigation of branching ratios and  $\gamma$ -ray emissions is still needed. In particular, single- $\gamma$ -ray emission is frequently used to assess sample activities, for example prior to shipping radioactive material. In the 2020 MEDICIS campaign, several samples were shipped from CERN to KU Leuven for research purpose [12]. However, the activities between what had been shipped and what was received disagreed, as branching ratios of questionable accuracy were used. From having received the sample, measurements with complementary techniques were used:  $\alpha$ -decay spectrometry, single- $\gamma$ -ray spectroscopy, and  $90^\circ$ -coincidence- $\gamma$ -ray spectroscopy on the same samples. Those techniques are more rudimentary than those applied for the half-life measurements, however they are also more likely to be used in day-to-day practice than the advanced techniques

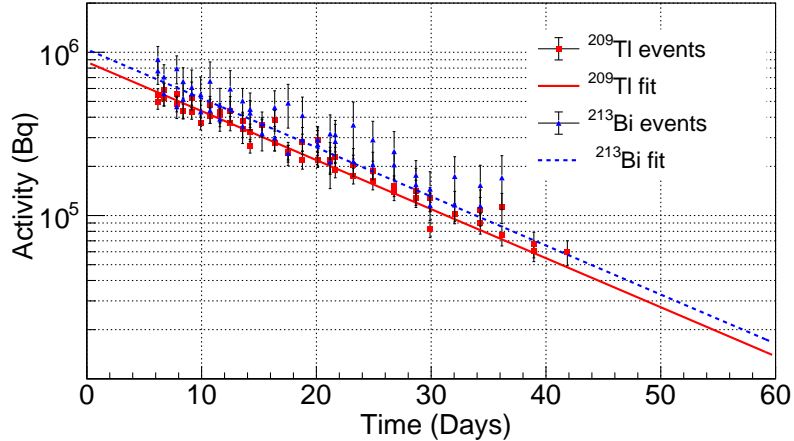


Figure 2: Activity extracted from the  $\gamma\gamma$  coincidences in  $^{213}\text{Bi}$  and  $^{209}\text{Tl}$  from the decay of  $^{225}\text{Ac}$  collected at MEDICIS and measured with two germanium detectors at  $90^\circ$ . The data are not corrected according to the multiplicities of the transitions, so that in particular the data from  $^{209}\text{Tl}$ , which weigh most on the combined statistics, cannot be used to extract accurate activities.

applied by metrology institutes. The conclusions of this investigation was that none of the activity measurements coincided and that large uncertainties were induced by the limited knowledge of the  $\beta$ - and  $\gamma$ -decay branching ratios [15].

In particular, there are very few  $\gamma\gamma$  cascades in the full decay chain, with limited knowledge on their branching ratios, so that the coincidence measurements are particularly challenging. From the two  $\gamma\gamma$  cascades identified of interest for MED024, one had an unknown multipolarity sequence through which it was not possible to correct for the  $90^\circ$  geometry and the data could not be used - see discrepancy on Fig. 2.

In light of these discrepancies, it is essential to investigate the entire decay chain to obtain reliable decay information, and in particular branching ratios and angular distributions from which to determine the multipolarity of transitions involved in  $\gamma\gamma$  cascades. All existing investigations on these isotopes stem from studies based on  $^{229}\text{Th}$  or  $^{225}\text{Ac}$  samples but rarely on the independent investigations of the isotopes directly [16, 17]. In order to avoid issues with  $\gamma$ -ray emissions overlapping between different isotopes along the decay chain, it is proposed to perform spectroscopy of the five main isotopes of the decay chain independently:  $^{225}\text{Ac}$ ,  $^{221}\text{Fr}$ ,  $^{217}\text{At}$ ,  $^{213}\text{Bi}$ , and  $^{209}\text{Tl}$ .

## 2.1 Decay of $^{225}\text{Ac}$

$^{225}\text{Ac}$  is the most bound  $A = 225$  isobar but is however not stable against  $\alpha$  decay and has a half-life of  $T_{1/2} = 9.9179(30)$  days. It means that its decay goes 100% via  $\alpha$  decay to  $^{221}\text{Fr}$ . While most of the decay goes directly to the ground state of the daughter nucleus, some of the population goes to excited states in  $^{221}\text{Fr}$  with many different  $\gamma$  rays emitted; however, the most intense transition, highlighted in Fig. 3, is at 99.8 keV with an absolute

$\gamma$ -ray intensity of about 1 emission per 100 decays. This is a rather weak emission at an energy that is also easily absorbed by packaging material (e.g. when characterising a sample for transport) and as such is not useful to quantify this isotope production.

## 2.2 Decay of $^{221}\text{Fr}$

$^{221}\text{Fr}$  has a half-life of  $T_{1/2} = 4.801(6)$  min and decays also mostly via  $\alpha$  decay to  $^{217}\text{At}$  ( $b_\alpha > 99.9\%$ ). Similar to its mother, this decay mostly proceeds from ground state to ground state, however, some  $\gamma$  rays are also emitted from excited states populated from the fine structure decays, see Fig. 4. Of particular interest is the  $\gamma$  ray emission at 218 keV, which occurs with an intensity of 11.44(12) per 100 decays, though a recent study starting from  $^{229}\text{Th}$  quotes for this transition an intensity of 12.57(30) per 100 decays [16], which is more than  $2\sigma$  off. This is one of the main transitions used to quantify the production of  $^{225}\text{Ac}$  with single- $\gamma$ -ray spectroscopy, e.g. for transport of radioisotopes, and its intensity should therefore be known accurately, ideally from a direct decay study with minimal background from other decays.

## 2.3 Decay of $^{217}\text{At}$

$^{217}\text{At}$  is a very short-lived isotope ( $T_{1/2} = 32.3(4)$  ms) and is a pure  $\alpha$  emitter decaying to  $^{213}\text{Bi}$ . Its decay goes almost entirely from ground state to ground state, so that none of the  $\gamma$  rays emitted in its decay have a sufficient intensity to be relevant for quantification, see Fig. 5.

## 2.4 Decay of $^{213}\text{Bi}$

$^{213}\text{Bi}$  is one of the most important isotopes in the decay chain of  $^{225}\text{Ac}$ , as it may also be used for medical applications, but also because its decay properties are important for quantitative analysis. Its half-life is  $T_{1/2} = 45.60(9)$  min and its decay goes either via  $\alpha$  decay to  $^{209}\text{Tl}$  ( $b_\alpha = 2.14(1)\%$ ) or  $\beta^-$  decay to  $^{213}\text{Po}$  ( $b_\beta = 97.86(1)\%$ ). This latter decay mode gives rise to the most intense  $\gamma$ -ray emission in the entire decay sequence, with a transition at 440.45(1) keV with an intensity of 25.94(15) per 100 decays, see Fig. 6. It also features one of the most intense  $\gamma\gamma$  cascades with energies 807.36 keV-292.80 keV and respective intensities 0.292(12) and 0.429(7) per 100 decays, which are two orders of magnitude down from the 440 keV single  $\gamma$  ray. It is also important to note that the multipolarity of the first transition at 807 keV is unknown while that of the second transition at 292 keV is a mixture of M1 and E2; as a consequence, this cascade cannot be used to determine efficiency-free activities with  $\gamma\gamma$  coincidences unless the full angular correlation can be measured, see the discrepancy in Fig. 2.

The decay of  $^{213}\text{Po}$  that follows is also a very fast decay ( $T_{1/2} = 3.72(2)$   $\mu\text{s}$ ) that proceeds via pure  $\alpha$  decay to  $^{209}\text{Pb}$ , almost entirely from ground state to ground state ( $I_\alpha = 99.9955(4)\%$ ).

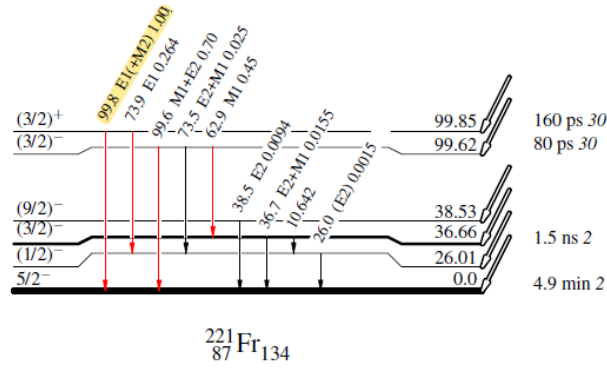


Figure 3: Extract from the  $\gamma$ -ray emission in the decay of  $^{225}\text{Ac}$ . The most intense line is highlighted in yellow ( $\gamma$ -ray intensity per 100 decays). Decays from higher levels are all under 0.1%.

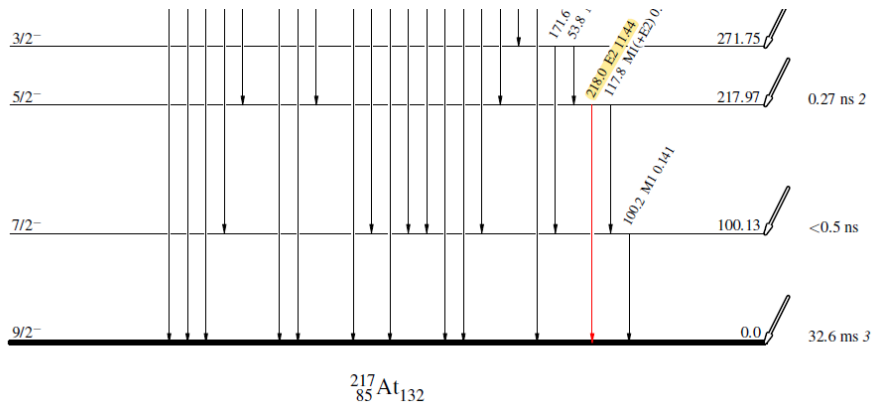


Figure 4: Extract from the  $\gamma$ -ray emission in the decay of  $^{221}\text{Fr}$ . The most intense line is highlighted in yellow ( $\gamma$ -ray intensity per 100 decays). Decays from higher levels are all under 0.1%.

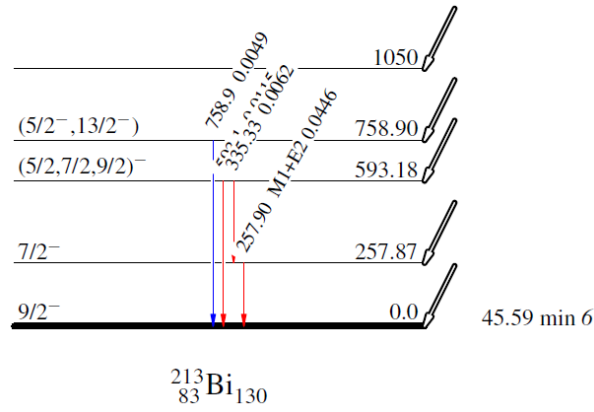


Figure 5: Gamma-ray emission in the decay of  ${}^{217}\text{At}$ . None of the lines are intense enough to be relevant in single- $\gamma$  or  $\gamma\gamma$ -ray spectroscopy ( $\gamma$ -ray intensity per 100 decays).

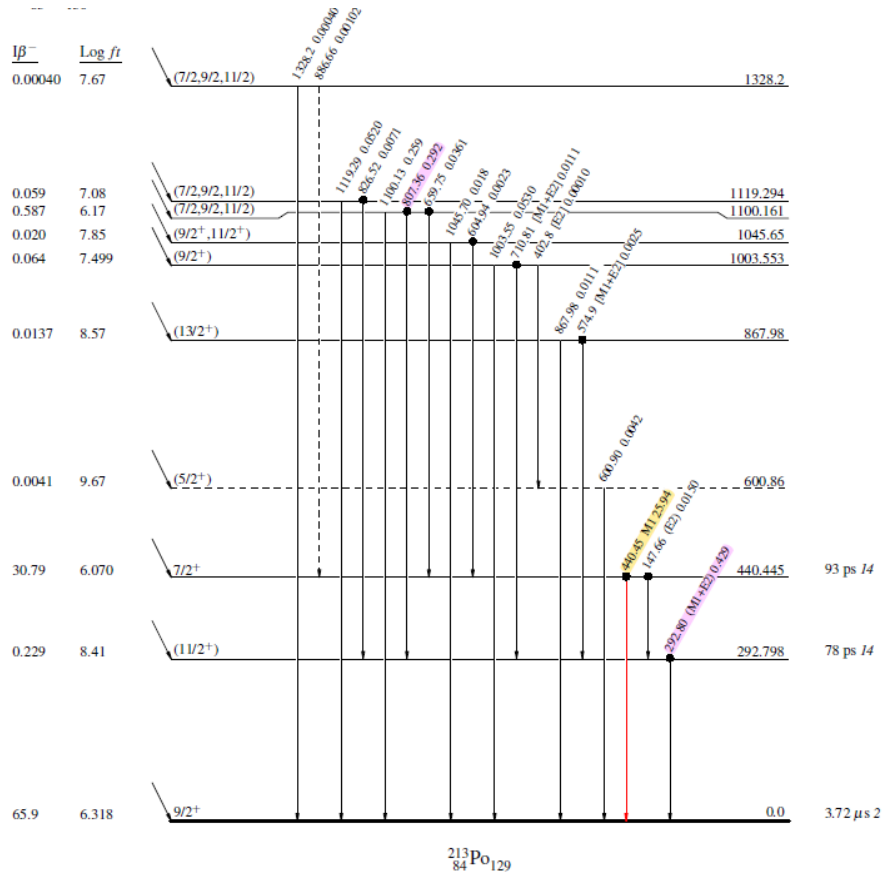


Figure 6: Gamma-ray emission in the decay of  ${}^{213}\text{Bi}$ . The most intense line is highlighted in yellow ( $\gamma$ -ray intensity per 100 decays) and the most intense  $\gamma\gamma$  cascade is highlighted in purple.



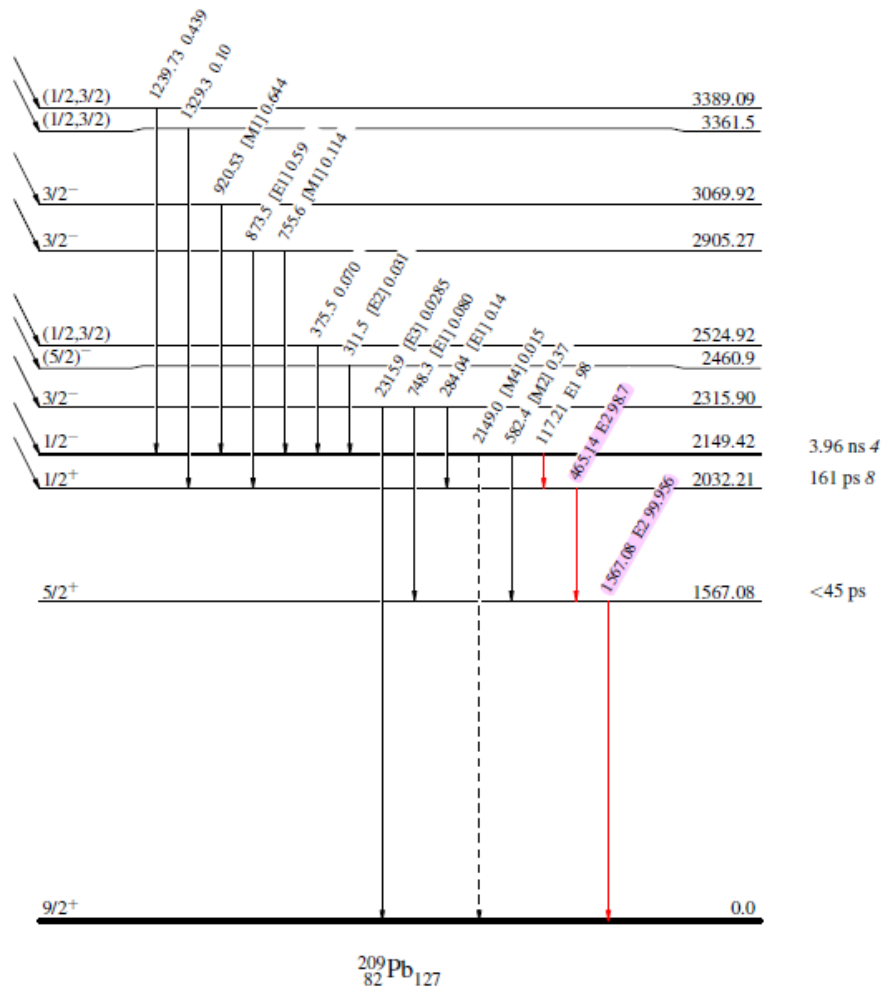


Figure 7: Gamma-ray emission in the decay of  $^{209}\text{Tl}$ . The most intense  $\gamma\gamma$  cascade is highlighted in purple. Due to the low  $\alpha$ -decay branching ratio in  $^{213}\text{Bi}$ , this isotope is not produced much so that its  $\gamma$ -ray lines are not prominent in the single- $\gamma$ -ray spectrum.

## 2.5 Decay of $^{209}\text{Tl}$

Although its population in the decay chain is limited by the  $\alpha$  branching ratio in the decay of  $^{213}\text{Bi}$  ( $b_\alpha = 2.14(1)\%$ ), this isotope remains very interesting in the quantification of the activity in the decay chain. It has a half-life of  $T_{1/2} = 2.162(3)$  min and decays exclusively via  $\beta^-$  decay to  $^{209}\text{Pb}$ , yielding in particular a  $\gamma\gamma$  cascade at energies 465.14(1) keV-1567.08(2) keV and respective intensities 95.4(10) and 99.663(7) per 100 decays; with all decays from the first transition proceeding via the second one. Moreover, this cascade is a pure E2-E2 sequence, so that it may be used very reliably for efficiency-free activity quantification, in spite of the low population of  $^{209}\text{Tl}$  in the decay chain.

## 3 Measurement at IDS

The ISOLDE Decay Station (IDS) is a permanent setup at ISOLDE that is also modular and allows for coincident charged-particles and  $\gamma$ -ray spectroscopy. The beam is delivered from ISOLDE and implanted on an aluminized Mylar tape that allows the frequent removal of long-lived activity building up in the decay chain. For this experiment, the setup will feature both a plastic scintillator (forward direction) and an annular silicon detector (backward direction) for detecting  $\beta^-$  and  $\alpha$  particles, with respective efficiencies of 40% and 15%, and an array of high-purity germanium clover detectors, with total singles efficiency of 6.4% at 1 MeV (12 clover configuration) and  $\gamma\gamma$  efficiency of 0.4% for performing angular correlation investigations for the study of multipolarities. Thanks to the new support structure with fully adjustable detector positions and increased number of HPGe detectors, a significant increase of statistics is expected compared to the old configuration [18].

The IDS setup is particularly well suited to study short-lived radioisotopes directly delivered from ISOLDE, such as  $^{221}\text{Fr}$ ,  $^{213}\text{Bi}$  and  $^{209}\text{Tl}$ , but may also be used to study longer-lived isotopes, such as  $^{225}\text{Ac}$ , by accumulating a sample without moving the tape and then performing a long-term study of its decay, first as it reaches equilibrium between the different isotopes in the progeny, and from there on. It is thus proposed to perform a dedicated decay spectroscopy of each of these four isotopes independently so that we may disentangle fully the impact of each decay on the total decay chain, by collecting a self-consistent set of data sets.

## 4 Beam time request

Beams of  $^{225}\text{Ac}$ ,  $^{221}\text{Fr}$ ,  $^{213}\text{Bi}$  and  $^{209}\text{Tl}$  have already been produced successfully at CERN ISOLDE from a  $\text{UC}_x$  target and the yields are presented in Table 1.  $^{221}\text{Fr}$  is easily produced with surface ionization,  $^{209}\text{Tl}$  may also be surface ionized but can also be enhanced with RILIS, finally  $^{225}\text{Ac}$  and  $^{213}\text{Bi}$  require RILIS for ionization.  $^{225}\text{Ac}$  may also be produced as a molecular beam of  $\text{AcF}_2$ , which is free of isobaric  $^{225}\text{Ra}$ . Due to its long half-life,  $^{225}\text{Ac}$  will remain at a low online activity, though an activity of  $7 \times 10^5$  Bq/ $\mu\text{C}$  would already be reached at the end of a shift. Altogether, the high production rate at ISOLDE enables a very fast collection of high statistics.

Isotope	Half-life	Yield [ $\mu\text{C}^{-1}$ ]	Shifts
$^{225}\text{Ac}$	9.9179(30) days	$3 \times 10^7$	1
$^{221}\text{Fr}$	4.801(6) min	$2.8 \times 10^7$	0.5
$^{213}\text{Bi}$	45.60(9) min	$5 \times 10^3$	1
$^{209}\text{Tl}$	2.162(3) min	$5 \times 10^4$	1

Table 1: Half-life and yields of the isotopes of interest, together with the requested beam time for each.

**Summary of requested shifts:** 3.5 shifts are requested for the collection and study of  $^{225}\text{Ac}$ ,  $^{221}\text{Fr}$ ,  $^{213}\text{Bi}$  and  $^{209}\text{Tl}$  to study their decay properties in isolation and understand the full decay chain from  $^{225}\text{Ac}$  towards its use in medical applications.

A key aspect of this proposal is the consistency between the different data sets, as the heaviest isotopes decay towards the lighter ones, as well as the use of a single detection system (IDS) to avoid systematic effects across multiple setups. This ensures that the data sets can thus be compared directly. If the data were collected over multiple runs, this would require cross calibration of the runs, easily achieved by collecting systematically data on  $^{221}\text{Fr}$ .

## References

- [1] J. Elgqvist, S. Frost, J.-P. Pouget, and P. Albertsson. The potential and hurdles of targeted alpha therapy - clinical trials and beyond. *Frontiers in Oncology*, 3:324, 2014.
- [2] C. Parker, S. Nilsson, D. Heinrich, S. I. Helle, J. M. O’Sullivan, S. D. Fossa, A. Chodacki, P. Wiechno, J. Logue, M. Seke, A. Widmark, D. C. Johannessen, P. Hoskin, D. Bottomley, N. D. James, A. Solberg, I. Syndikus, J. Kliment, S. Wedel, S. Boehmer, M. Dall’Oglio, L. Franzén, R. Coleman, N. J. Vogelzang, C. G. O’Byrne-Tear, K. Staudacher, J. Garcia-Vargas, M. Shan, O. S. Bruland, and O. Sartor. Alpha emitter radium-223 and survival in metastatic prostate cancer. *The New England Journal of Medicine*, 369:213–223, 2013.
- [3] M. Shirley and P. L. McCormack. Radium-223 dichloride: a review of its use in patients with castration-resistant prostate cancer with symptomatic bone metastases. *Drugs*, 74:579–586, 2014.
- [4] M. R. McDevitt, D. Ma, J. Simon, R. K. Frank, and S. A. Scheinberg. Design and synthesis of  $^{225}\text{Ac}$  radioimmunopharmaceuticals. *Applied Radiation and Isotopes*, 57:841–847, 2002.
- [5] Mn. Makvandi, E. Dupis, J. W. Engle, F. M. Nortier, M. E. Fassbender, S. Simon, E. R. Birnbaum, R. W. Atcher, K. D. John, O. Rixe, and J. P. Norenberg. Alpha-emitters and targeted alpha therapy in oncology: from basic science to clinical investigations. *Targeted Oncology*, 13:189–203, 2018.

- [6] S. Ahenkora, I. Cassells, C. M. Deroose, T. Cardinaels, A. R. Burgoyne, G. Bormans, Ooms. M., and F. Cleeren. Bismuth-213 for targeted radionuclide therapy: from atom to bedside. *Pharmaceutics*, 13:599, 2021.
- [7] A. Morgenstern, F. Bruchertseifer, and C. Apostolidis. Bismuth-213 and actinium-225 - generator performance and evolving therapeutic applications in two generator-derived alpha-emitting radioisotopes. *Current Radiopharmaceuticals*, 5:221–227, 2012.
- [8] C. Krachtowil, F. Bruchertseifer, F. L. Giesel, M. Weis, F. A. Verburg, F. Mottaghy, K. Kopka, C. Apostolidis, U. Haberkorn, and A. Morgenstern.  $^{225}\text{Ac}$ -PSMA-617 for PSMA-targeted  $\alpha$ -radiation therapy of metastatic castration-resistant prostate cancer. *The Journal of Nuclear Medicine*, 57:1941–1944, 2016.
- [9] C. Krachtowil, U. Haberkorn, and F. L. Giesel.  $^{225}\text{Ac}$ -PSMA-617 for therapy of prostate cancer. *Seminars in Nuclear Medicine*, 50:133–140, 2020.
- [10] F. Bruchertseifer, A. Kellerbauer, R. Malmbeck, and A. Morgenstern. Targeted alpha therapy with bismuth-213 and actinium-225: meeting future demand. *Journal of Labelled Compounds and Radiopharmaceuticals*, 62:794–802, 2019.
- [11] K. Dockx et al. IS637: Towards reliable production of  $^{225}\text{Ac}$  for medical applications: systematic analysis of the production of Fr, Ra and Ac beams. INTC proposal INTC-P-498, CERN, 2017.
- [12] T. E. Cocolios et al. MED024: Mass separation of  $^{225}\text{Ac}$  from  $^{227}\text{Ac}$  and from irradiated Th targets to support targeted alpha therapy. MEDICIS proposal MED-024, CERN, 2020.
- [13] T. E. Cocolios, F. Cleeren, et al. MED030: Targeted alpha therapy research in Belgium: qualifying the  $^{225}\text{Ac}$  pipeline. MEDICIS proposal MED-030, CERN, 2021.
- [14] S. Pommé, M. Marouli, G. Suliman, H. Dikmen, R. Van Ammel, V. Jobbágy, A. Dirican, H. Stroh, J. Paepen, F. Bruchertseifer, C. Apostolidis, and A. Morgenstern. Measurement of the  $^{225}\text{Ac}$  half-life. *Applied Radiation and Isotopes*, 70:2608–2614, 2012.
- [15] M. Heines. Mass separation of  $^{225}\text{Ac}$  for medical applications: first proof of principle at CERN-MEDICIS. Master’s thesis, KU Leuven, 2021.
- [16] R. S. Gomes, J. U. Delgado, da Silva C. J., P. A. L. da Cruz, A. L. Ferreira Filho, M. C. M. de Almeida, A. Iwahara, A. E. de Oliveire, and L. Tauhata. Measurement of the absolute gamma emission intensities from the decay of Th-229 in equilibrium with progeny. *Applied Radiation and Isotopes*, 166:190323, 2020.
- [17] M. P. Takács and K. Kossert. Half-life determination of  $^{213}\text{Bi}$  and  $^{209}\text{Pb}$  by means of Cherenkov counting and detection with a NaI detector. *Applied Radiation and Isotopes*, 167:109425, 2021.

- [18] T. A. Berry et al. Octupole states in  $^{207}\text{Tl}$  studied through  $\beta$  decay. *Physical Review C*, 101:054311, May 2020.

# Appendix

## DESCRIPTION OF THE PROPOSED EXPERIMENT

The experimental setup comprises: (*name the fixed-ISOLDE installations, as well as flexible elements of the experiment*)

Part of the	Availability	Design and manufacturing
(if relevant, name fixed ISOLDE installation: COLLAPS, CRIS, ISOLTRAP, MINIBALL + only CD, MINIBALL + T-REX, NICOLE, SSP-GLM chamber, SSP-GHM chamber, or WITCH)	<input checked="" type="checkbox"/> Existing	<input checked="" type="checkbox"/> To be used without any modification
[Part 1 of experiment/ equipment]	<input type="checkbox"/> Existing	<input type="checkbox"/> To be used without any modification <input type="checkbox"/> To be modified
	<input type="checkbox"/> New	<input type="checkbox"/> Standard equipment supplied by a manufacturer <input type="checkbox"/> CERN/collaboration responsible for the design and/or manufacturing
[Part 2 of experiment/ equipment]	<input type="checkbox"/> Existing	<input type="checkbox"/> To be used without any modification <input type="checkbox"/> To be modified
	<input type="checkbox"/> New	<input type="checkbox"/> Standard equipment supplied by a manufacturer <input type="checkbox"/> CERN/collaboration responsible for the design and/or manufacturing
[insert lines if needed]		

HAZARDS GENERATED BY THE EXPERIMENT (if using fixed installation:) Hazards named in the document relevant for the fixed [COLLAPS, CRIS, ISOLTRAP, MINIBALL + only CD, MINIBALL + T-REX, NICOLE, SSP-GLM chamber, SSP-GHM chamber, or WITCH] installation.

Additional hazards:

Hazards	[Part 1 of experiment/ equipment]	[Part 2 of experiment/ equipment]	[Part 3 of experiment/ equipment]
<b>Thermodynamic and fluidic</b>			
Pressure	[pressure][Bar], [volume][l]		
Vacuum			
Temperature	[temperature] [K]		
Heat transfer			
Thermal properties of materials			
Cryogenic fluid	[fluid], [pressure][Bar], [volume][l]		

<b>Electrical and electromagnetic</b>			
Electricity	[voltage] [V], [current][A]		
Static electricity			
Magnetic field	[magnetic field] [T]		
Batteries	<input type="checkbox"/>		
Capacitors	<input type="checkbox"/>		
<b>Ionizing radiation</b>			
Target material [material]			
Beam particle type (e, p, ions, etc)			
Beam intensity			
Beam energy			
Cooling liquids	[liquid]		
Gases	[gas]		
Calibration sources:	<input type="checkbox"/>		
• Open source	<input type="checkbox"/>		
• Sealed source	<input type="checkbox"/> [ISO standard]		
• Isotope			
• Activity			
Use of activated material:			
• Description	<input type="checkbox"/>		
• Dose rate on contact and in 10 cm distance	[dose][mSV]		
• Isotope			
• Activity			
<b>Non-ionizing radiation</b>			
Laser			
UV light			
Microwaves (300MHz-30 GHz)			
Radiofrequency (1-300 MHz)			
<b>Chemical</b>			
Toxic	[chemical agent], [quantity]		
Harmful	[chem. agent], [quant.]		
CMR (carcinogens, mutagens and substances toxic to reproduction)	[chem. agent], [quant.]		
Corrosive	[chem. agent], [quant.]		
Irritant	[chem. agent], [quant.]		
Flammable	[chem. agent], [quant.]		

Oxidizing	[chem. agent], [quant.]		
Explosiveness	[chem. agent], [quant.]		
Asphyxiant	[chem. agent], [quant.]		
Dangerous for the environment	[chem. agent], [quant.]		
<b>Mechanical</b>			
Physical impact or mechanical energy (moving parts)	[location]		
Mechanical properties (Sharp, rough, slippery)	[location]		
Vibration	[location]		
Vehicles and Means of Transport	[location]		
<b>Noise</b>			
Frequency	[frequency],[Hz]		
Intensity			
<b>Physical</b>			
Confined spaces	[location]		
High workplaces	[location]		
Access to high workplaces	[location]		
Obstructions in passageways	[location]		
Manual handling	[location]		
Poor ergonomics	[location]		

Hazard identification:

Average electrical power requirements (excluding fixed ISOLDE-installation mentioned above): [make a rough estimate of the total power consumption of the additional equipment used in the experiment]